term, $-k[\mathrm{B}][\mathrm{P}(\mathbf{r})]$, corresponds to an induced screening charge in a conducting medium. For a uniform concentration of protease, the long-range $1/r$ potential is reduced exponentially:

$$\phi(r)=1/r\rightarrow\phi_{\mathrm{scr}}(r)=(1/r)\exp(-r/\lambda)$$

and $\lambda^2=D/k[\mathrm{B}]$.

In simple terms, degradation by the protease limits the size of the pheromone cloud around each α-cell to a radius λ, the average distance that a pheromone molecule diffuses before being degraded. This screening increases the alignment between the gradient and the direction to the nearest mating partner, although the gradient strength is reduced (Fig. 1b,c). Consequently, the protease is not helpful when there is only a single source of pheromone, as was observed by Segall[3]. Effective screening is obtained when λ is of the order of the mean distance between cells (about 10 μm), which for a diffusion-limited process indicates a protease concentration of about 1 nM.

For simplicity, we assumed uniform protease concentration when deriving the last equation. However, our results generalize to non-uniform conditions provided that the protease is present over a range corresponding to several intercell distances around the **a**-cell. This is likely to occur, as protease-secreting **a**-cells are distributed throughout the population and the protease is a stable, widely diffusing molecule[4,8].

Mechanisms that screen concentration gradients may be more generally applicable. Cells of mating type α may have an activity that inactivates **a**-factor[9]. Screening may also be used in chemotaxis; for example, the slime mould *Dictyostelium* secretes factors that antagonize the attractants cyclic AMP and folate. The effective range of signalling by diffusible growth factors may also be regulated by a similar mechanism. For example, the growth factor Spitz is inhibited in the developing *Drosophila* eye[10]. Studies of model systems, such as that discussed here, may provide a better understanding of the quantitative effects of mechanisms that control the range of signalling.

**Naama Barkai*†, Mark D. Rose†,
Ned S. Wingreen‡**

*Departments of *Physics and †Molecular Biology,
Princeton University,
Princeton, New Jersey 08544, USA*
‡*NEC Research Institute,
4 Independence Way,
Princeton, New Jersey 08540, USA
e-mail: wingreen@research.nj.nec.com*

1. Jackson, C. & Hartwell, L. H. *Cell* **63**, 1039–1051 (1990).
2. Jackson, C. & Hartwell, L. H. *Mol. Cell. Biol.* **10**, 787–796 (1990).
3. Segall, J. E. *Proc. Natl Acad. Sci. USA* **90**, 8332–8336 (1993).
4. Hicks, J. B. & Herskowitz, I. *Nature* **260**, 246–248 (1976).
5. Ciejek, E. & Thorner, J. *Cell* **18**, 623–635 (1979).
6. Sprague, G. F. & Herskowitz, I. *J. Mol. Biol.* **153**, 305–321 (1981).
7. Chan, R. K. & Otte, C. A. *Mol. Cell. Biol.* **2**, 11–20 (1982).
8. Manney, T. R. *J. Bacteriol.* **155**, 291–301 (1983).
9. Steden, M., Betz, R. & Duntze, W. *Mol. Gen. Genet.* **219**, 439–444 (1989).
10. Wasserman, D. & Freeman, M. *Trends Cell Biol.* **7**, 431–436 (1997).

Robust dinosaur phylogeny?

The Ankylosauria comprises two families of armoured dinosaurs (Nodosauridae and Ankylosauridae) that are best known from well-preserved specimens from the Cretaceous period. In their report on the skull of a new Jurassic ankylosaur, *Gargoyleosaurus*, Carpenter *et al.*[1] presented a phylogenetic analysis of four terminal taxa, which yielded a tree with *Gargoyleosaurus* as the sister taxon of the Ankylosauridae. But the authors' claim that their tree is robust is undermined when their data and their tree are evaluated using numerical techniques.

Although Carpenter *et al.*'s preferred tree (Fig. 1a) is the most parsimonious tree for their data, the alternatives in which *Gargoyleosaurus* is the sister taxon of either the Nodosauridae (Fig. 1b) or Nodosauridae + Ankylosauridae (Fig. 1c) are only slightly less parsimonious. Of their 26 characters, just six support their preferred tree, four support *Gargoyleosaurus* + Nodosauridae, and two support Nodosauridae and Ankylosauridae. The remaining 14 characters are phylogenetically uninformative.

The 'winning sites' test[2] shows that the differences between Carpenter *et al.*'s preferred tree and the slightly less parsimonious alternatives shown in Fig. 1b and c are not significant (P values of 0.75 and 0.29, respectively), so they do not allow us to identify any tree as being significantly better supported by the data than any other. Similarly, bootstrap support for the association of *Gargoyleosaurus* and the Ankylosauridae is not compelling (71%, 2,000 replicates). Matrix randomization tests also indicate the limitations of the data. Permutation tail probabilities for the data based on parsimony tree length[3] and pairwise character compatibilities[4,5] are 0.51 and 0.43, respectively, and do not allow us to reject the null hypothesis that congruence within the data is no greater than expected by chance alone.

Taken together, these results indicate that Carpenter *et al.*'s claim that their preferred tree is robust is not justified. Their conclusions may also be undermined by their use of aggregate in-group terminal taxa (nodosaurids and ankylosaurids), which precludes the placement of *Gargoyleosaurus* within either of these clades. Consequently, a phylogenetically important position for *Gargoyleosaurus* as sister taxon to a major clade is inevitable.

Choice of taxa also has an effect on the character evidence. The assumed plesiomorphic condition of character 22 (a 'neck' at the base of the occipital condyle),
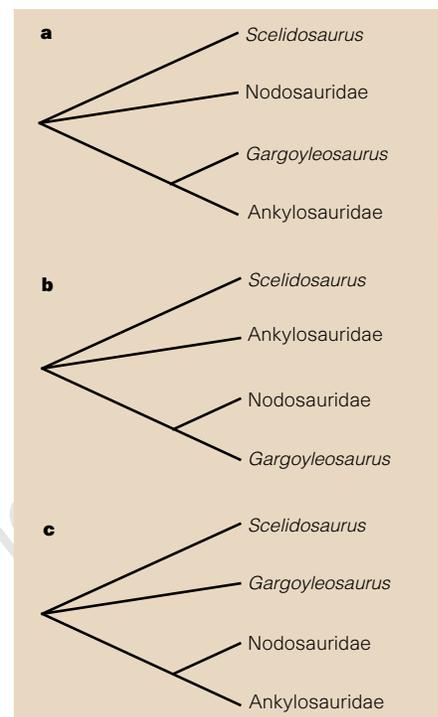
Figure 1 The three possible trees of ankylosaur relationships (rooted on *Scelidosaurus* with the basal polytomy unresolved). **a,** Tree based on the data of Carpenter *et al.*[1], which is the most parsimonious tree (tree length of 32 steps); **b,** the next most parsimonious tree (tree length of 34 steps); **c,** the least parsimonious tree (tree length of 36 steps).

one of the six characters used to support *Gargoyleosaurus* + Anklyosauridae, is present in several ankylosaurids (for example, *Talarurus*, *Tarchia* and *Maleevus*)[6]. Recoding this character as polymorphic for the aggregate Ankylosauridae reduces the number of potential synapomorphies for *Gargoyleosaurus* + Ankylosauridae to just five, and highlights the possibility that *Gargoyleosaurus* might nest within the Ankylosauridae.

Carpenter *et al.*[1] noted that strong brain flexure in *Gargoyleosaurus* is shared with at least some nodosaurids, but they interpreted this similarity as primitive because the ornithopod *Hypsilophodon* has a similar condition. In contrast, comparison with Stegosauria, a more proximate outgroup, suggests that this similarity is derived within Ankylosauria, increasing the evidence for *Gargoyleosaurus* + Nodosauridae to five potential synapomorphies. That these minor revisions to the character data can render the hypotheses represented in Fig. 1a and b equally parsimonious underscores the frailty of the data and the phylogenetic conclusions.

Gargoyleosaurus may well be an ankylosaurid, but this inference has not yet been demonstrated. Robust resolution of the phylogenetic placement of *Gargoyleosaurus* and assessment of its implications for the evolution of Ankylosauria will require a

thorough analysis of a more comprehensive data set.

**Mark Wilkinson*†, Paul Upchurch*,
Paul M. Barrett‡, David J. Gower§,
Michael J. Benton§**
**School of Biological Sciences,
University of Bristol,
Bristol BS8 1UG, UK*
†*Department of Zoology,
Natural History Museum,
London SW7 5BD, UK*
‡*Department of Earth Sciences,
University of Cambridge,
Cambridge CB2 3EQ, UK*
§*Department of Earth Sciences,
University of Bristol,
Bristol BS8 1RJ, UK*

1. Carpenter, K., Miles, C. & Cloward, K. *Nature* **393**, 782–783 (1998).
2. Prager, E. M. & Wilson, A. C. *J. Mol. Evol.* **27**, 326–325 (1988).
3. Faith, D. P. & Cranston, P. S. *Cladistics* **7**, 1–28 (1991).
4. Alroy, J. *Syst. Biol.* **43**, 430–437 (1994).
5. Wilkinson, M. *Biol. Rev.* **7**, 423–470 (1997).
6. Barrett, P. M., Hailu, Y., Upchurch, P. & Burton, A. C. *J. Vert. Paleontol.* **18**, 376–384 (1998).

Moving ahead through differential visual latency

The time it takes to transmit information along the human visual pathways introduces a substantial delay in the processing of images that fall on the retina. This visual latency might be expected to cause a moving object to be perceived at a position behind its actual one, disrupting the accuracy of visually guided motor actions such as catching or hitting, but this does not happen. It has been proposed that the perceived position of a moving object is extrapolated forwards in time to compensate for the delay in visual processing[1–3].

We have studied the spatial misalignment perceived between moving and strobed objects and find that it varies systematically with the luminance of the objects. Our results favour an explanation for these perceived misalignments based on differential visual latencies, rather than on motion extrapolation. Thus, accurate visually guided motor actions are likely to depend on motor instead of perceptual compensation.

Evidence for a mechanism based on motion extrapolation[1–3] comes from the flash–lag phenomenon[4], in which a continuously moving object is perceived to be ahead of a stationary strobed object when the two retinal images are physically aligned. But because visual latency varies according to the properties of a stimulus, including its luminance[5–9], this mechanism would have to compensate appropriately for a range of stimulus-dependent variations in latency to ensure that real-time, visually guided responses are accurate. An alternative, previous

explanation, invoking a longer delay for the processing of a flashing stimulus, was based on attentional mechanisms[10].

According to the hypothesis based on differential visual latencies, the observed spatial lead of the moving central segment in Fig. 1a is directly proportional to the difference between the latencies of the strobed and the moving central segments. For a given stimulus, the visual latency varies inversely with its luminance[5–9], so the observed spatial lead in the flash–lag paradigm should vary according to the luminance of the strobed and moving central segments. Increasing the luminance of the moving central segments but not that of the strobed segments should decrease the delay of the moving central segment (d_m) while

Figure 1 Luminance-dependent misalignments between moving and strobed targets. **a,** The stimulus was a continuously rotating central segment (40 rev min⁻¹) and two flanking strobed segments (5 ms). **b,** The observed temporal lead of the moving central segment is shown as a function of its detectability (0=threshold) for three subjects (S.S.P., G.P. and T.L.N.). Positive values on the *y*-axis represent a temporal lead in perceiving the moving central segment relative to the strobed segments. The observed spatial lead was converted into a temporal lead by dividing it by the velocity of the moving central segment. **c,** The observed temporal lead of the moving central segment is shown as a function of the detectability of the strobed segments (0=threshold) for the same subjects.

that of the strobed segment (d_s) remains constant. The latency-difference hypothesis therefore predicts that the observed spatial lead of the moving central segment should increase.
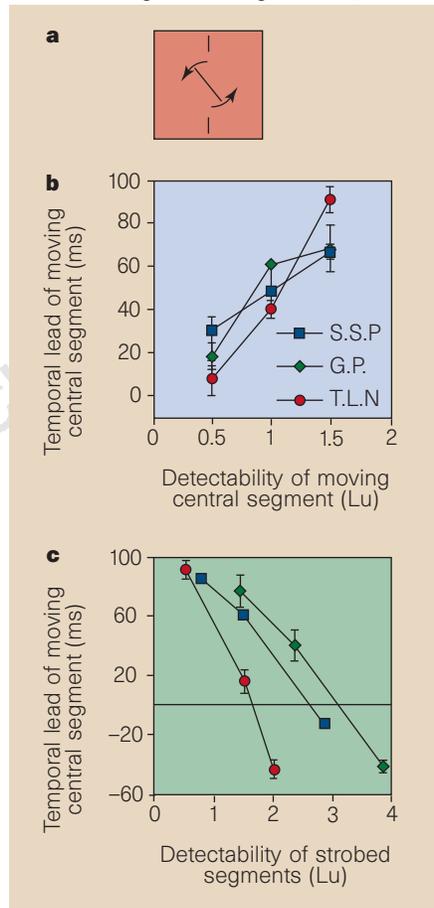
To test this prediction, we measured the spatial lead of the moving central segment as a function of the detectability of the central segment while keeping the detectability of the strobed segments constant. Here we use detectability to refer to the number of log units of luminance (Lu) above the detection threshold; detectability of the strobed segments was 0.3 Lu for subjects S.S.P. and G.P., and 0.5 Lu for T.L.N. The temporal lead of the moving central segment averaged across subjects increases systematically from 20 to 70 ms when its detectability increases by 1.0 Lu (Fig. 1b).

Increasing the luminance of the strobed segments while keeping that of the moving central segment constant should decrease d_s, while d_m remains constant. The latency-difference hypothesis predicts that the observed spatial lead of the moving central segment should decrease and, if the luminance of the strobed segments is high enough, the moving central segment should be perceived to lag behind spatially. We tested this prediction by measuring spatial lead as a function of the detectability of the strobed segments, while keeping the detectability of the moving central segment constant (1.5 Lu above the detection threshold for subjects G.P. and T.L.N., and 0.8 Lu for S.S.P.). The observed temporal lead of the moving central segment averaged across subjects decreases systematically from 80 to −30 ms as the detectability of the strobed segments increases by 1.5 to 2.0 Lu (Fig. 1c).

These results support predictions of the latency-difference hypothesis and show that the motion-extrapolation mechanism does not compensate for stimulus-dependent variations in latency. Indeed, theoretical calculations show that the putative motion-extrapolation mechanism must be undercompensating by at least 120 ms to account for the data in Fig. 1. But a motion-extrapolation mechanism that does not adequately compensate for variations in visual latency would not appreciably improve the accuracy of real-time visually guided behaviour.

**Gopathy Purushothaman*, Saumil S. Patel†,
Harold E. Bedell†, Haluk Ogmen***
**College of Engineering and* †*College of Optometry,
University of Houston,
Houston, Texas 77204, USA
e-mail: hbedell@uh.edu*

1. Nijhawan, R. *Nature* **370**, 256–257 (1994).
2. Nijhawan, R. *Nature* **386**, 66–69 (1997).
3. Khurana, B. & Nijhawan, R. *Nature* **378**, 566 (1995).
4. MacKay, D. M. *Nature* **181**, 507–508 (1958).
5. Bacon, F. *Novum Organum* (Bills, London, 1620).
6. Cattell, J. M. *Brain* **9**, 512–515 (1886).
7. Mansfield, R. J. W. *Vis. Res.* **13**, 2219–2234 (1973).
8. Roufs, J. A. J. *Vis. Res.* **14**, 853–869 (1974).
9. Williams, J. M. & Lit, A. *Vis. Res.* **23**, 171–179 (1983).
10. Baldo, M. V. C. & Klein, S. A. *Nature* **378**, 565–566 (1995).